Structural evaluation and protium-deuterium exchange in 1-ethyl-3-methylimidazolium halide-ethylene glycol mixtures

Zhengfei Chen[a,b], *Yuto Tonouchi*[b], *Kazuhiko Matsumoto*[b*], *Seiji Tsuzuki*[c], *Takashi Nagata*[d], *Masato Katahira*[d], *Rika Hagiwara*[b]

[a]School of Biological and Chemical Engineering, NingboTech University, Ningbo 315100, China

[b]Department of Fundamental Energy Science, Graduate School of Energy Science, Kyoto University, Yoshida, Sakyo-ku, Kyoto 606-8501, Japan

[c]Research Center for Computational Design of Advanced Functional Materials, National Institute of Advanced Industrial Science and Technology, Tsukuba, Ibaraki 305-8568, Japan

[d]Institute of Advanced Energy, Kyoto University, Uji, Kyoto 611-0011, Japan

Corresponding Author

*k-matsumoto@energy.kyoto-u.ac.jp (Kazuhiko Matsumoto)

Phone: +81-75-753-5827

Abstract

A series of equimolar mixtures of 1-ethyl-3-methylimidazolium halide ([C_2C_1im]X: X^- = F^-, Cl^-, Br^- and I^-) and ethylene glycol (EG) are studied by ^{1}H NMR and IR spectroscopies. The chemical shifts for the protons in EG and imidazolium ring shift towards the downfield in the order of F^- >> Cl^- > Br^- > I^-, owing to the strength of their respective X···H interactions. Amongst all the studied systems, the fluoride complex ([C_2C_1im]F·EG) shows extremely strong interactions between F^- and OH hydrogen of EG, resulting in no “free” EG in the mixture as reflected in the infrared spectra. Quantum chemical calculations suggest several possible geometries for all the halide systems, where the geometry with the EG molecule forming a chelate of halide ion gives the most stable structure. The calculated interaction energies of these geometries also confirm that the fluoride complex has a significantly higher interaction energy than those of the other halide systems. Furthermore, the halide anion affects the selectivity of protium-deuterium exchange site in these systems, and some imidazolium ring hydrogen atoms are activated only in the presence of F^-.

Keywords: Solvate ionic liquids; NMR spectroscopy; Protium-deuterium exchange; Theoretical calculations

1. Introduction

Ionic liquids (ILs) entirely composed of ionic species, very often containing an organic ion[1-4], are considered as “designer” solvents owing to their great tunability in physicochemical properties through structural modification of the cation or anion, leading to a wide range of applications in materials synthesis[5, 6], biomass processing[7], catalysis[1, 8], self-assembly[9, 10], and electrolytes for energy devices[11-14]. Solvate ionic liquids (SILs) are a subset of ILs, in which the cation (or anion) is solvated by a neutral species to form a stable complex cation (or anion) and the neutral species lose its properties as solvent[15]. Typical examples for SILs are those of lithium cation solvated by oligoethers (glymes)[16]. In the Li-glyme system including SILs, the interactions amongst the Li^+, anion and solvating neutral glymes play a crucial role in determining their structures[17-20], as examined by experimental and computational techniques[21]. The difference in nature of the solvation of Li^+ leads to many types of SILs that are defined as “good” or “poor”, depending on the ratio of glyme to Li^+ and relative coordination strengths of the glyme and anion with Li^+[18, 19, 22]. In a good SIL, Li-glyme complexation is favoured over the anion, giving properties similar to a conventional IL, while poor SILs are closer to a concentrated salt solution[23].

Our recent study reported that a fluoride anion solvated by ethylene glycol (EG)

formed room-temperature SILs with an appropriate cation[24]. The fluoride-based SILs, in which the fluoride ion was solvated by EG, was formed with the prototypical 1-alkyl-3-methylimidazolium cation ($[C_nC_1im]^+$)[24]. X-ray diffraction and nuclear magnetic resonance (NMR) and infrared (IR) spectroscopic studies showed that the fluoride ion had strong interactions with the OH groups in EG through H-bonding compared to the bromide system but it could interact with other hydrogen atoms in the cation. This phenomenon is similar to that in a typical deep eutectic solvent (DES), such as choline chloride-urea, in which multiple H-bonding interactions exist as revealed by computational simulations[25, 26]. Such a fluoride ion was termed as partially naked fluoride in comparison with practically naked fluoride in typical organic fluoride salts[27-30]. Different from naked fluoride ion that attacks most organic cation, fluoride ions solvated by EG do not decompose $[C_nC_1im]^+$. Interactions between fluoride and OH group in alcohols were comprehensively studied by X-ray diffraction and spectroscopic methods[31], and enhanced activity of the fluoride ion was confirmed for some fluorination reactions in the presence of H-bonding donors such as alcohols. Another work on fourteen different fluoride-alcohol complexes with bulky tetrabutylammonium cation revealed that the OH···F contacts in their crystal structures became shorter as the coordination number decreases and the O···F···O angle could be related to the reactivity of fluoride anion[32].

An IR and NMR spectroscopic study on H-bonding interactions in four imidazolium based ILs ([C_4C_1im]X, X=Cl, Br, I and BF_4) revealed that the anion greatly affects the stability of the H-bonding network, particularly on the isotopic protium-deuterium (^{1}H-^{2}H) exchanges between the H2 hydrogen on the imidazolium cation (H2 is the hydrogen atom on the carbon atom (C2) between two nitrogen atoms) and deuterium atom in ^2H_2O[33]. Deuteration is a chemical process used for minimal modification of molecules by replacing ^{1}H with ^{2}H. It is a powerful method in studying the structures of both existing and new molecules/materials[21, 34-39].

In the present work, the structures of [C_2C_1im]X·EG (X = F, Cl, Br, and I) mixtures in which the halide anion interacts with both EG and the cation are studied by the combination of experimental techniques (NMR and IR) and theoretical calculations. The effect of the anion size is readily reflected in the NMR and IR spectra, suggesting the H-bonding structure has changed accordingly, which is also reflected by the isotopic ^{1}H-^{2}H exchanges on both the EG and imidazolium ring.

2. Results and discussion

2.1. Solvation structures. Figure 1 shows the optimized structures of the [C_2C_1im]X·EG complexes (X = F, Cl, Br and I) and the calculated stabilization energies (E_{form}) associated with the formation of the complexes from isolated species (see the chemical structure in Figure 2 for the atom numbering scheme). The E_{form} calculated for

the most stable structure of the complex becomes smaller (less negative) with increasing anion size, due to the increased intermolecular distance, since the electrostatic and induction interactions are the major source of the attraction in the complexes. The E_{form} for the F^- complex is significantly smaller than that for the Cl^- complex, and then the E_{form} moderately increases afterwards (the E_{form} for the F^-, Cl^-, Br^- and I^- complexes are −134.7, −103.8, −103.4 and −94.0 kcal mol^{-1}, respectively). In the most stable structures for the four complexes, the two O−H hydrogen atoms of ethylene glycol have contacts with the halide anion, which suggests that the interaction between the O−H hydrogen and halide anion is important for the stabilization of the complexes. The E_{form} calculated for the $[C_2C_1im]X$ and $[EG]X^-$ complexes are summarized in Figure S1 in Supplementary data. In the absence of EG, a stable $[C_2C_1im]F$ complex does not exist. During the geometry optimization of the $[C_2C_1im]F$ complex, F^- abstracts H2 from $[C_2C_1im]^+$, which agrees with the experimental difficulty in the synthesis of pure $[C_2C_1im]F$ and the high basicity of naked F^-. On the other hand, stable geometries for the $[C_2C_1im]X$ (X = Cl, Br and I) were obtained by the geometry optimizations without EG. The E_{form} for the $[C_2C_1im]X$ complexes decreases (becomes less negative) with increasing the anion size. The bidentate structures for the $[EG]X^-$ complexes are more stable than the monodentate structures as shown in Figure S1. In the $[EG]X^-$ complexes, the $[EG]F^-$ has the largest negative

E_{form}. The absolute value of E_{form} calculated for the bidentate [EG]F^- (−45.5kcal mol^{-1}) is twice larger than that for the bidentate [EG]Cl^- complex (−19.5kcal mol^{-1}). The E_{form} for the [EG]X^- complexes monotonously decrease from Cl^- to I^-.

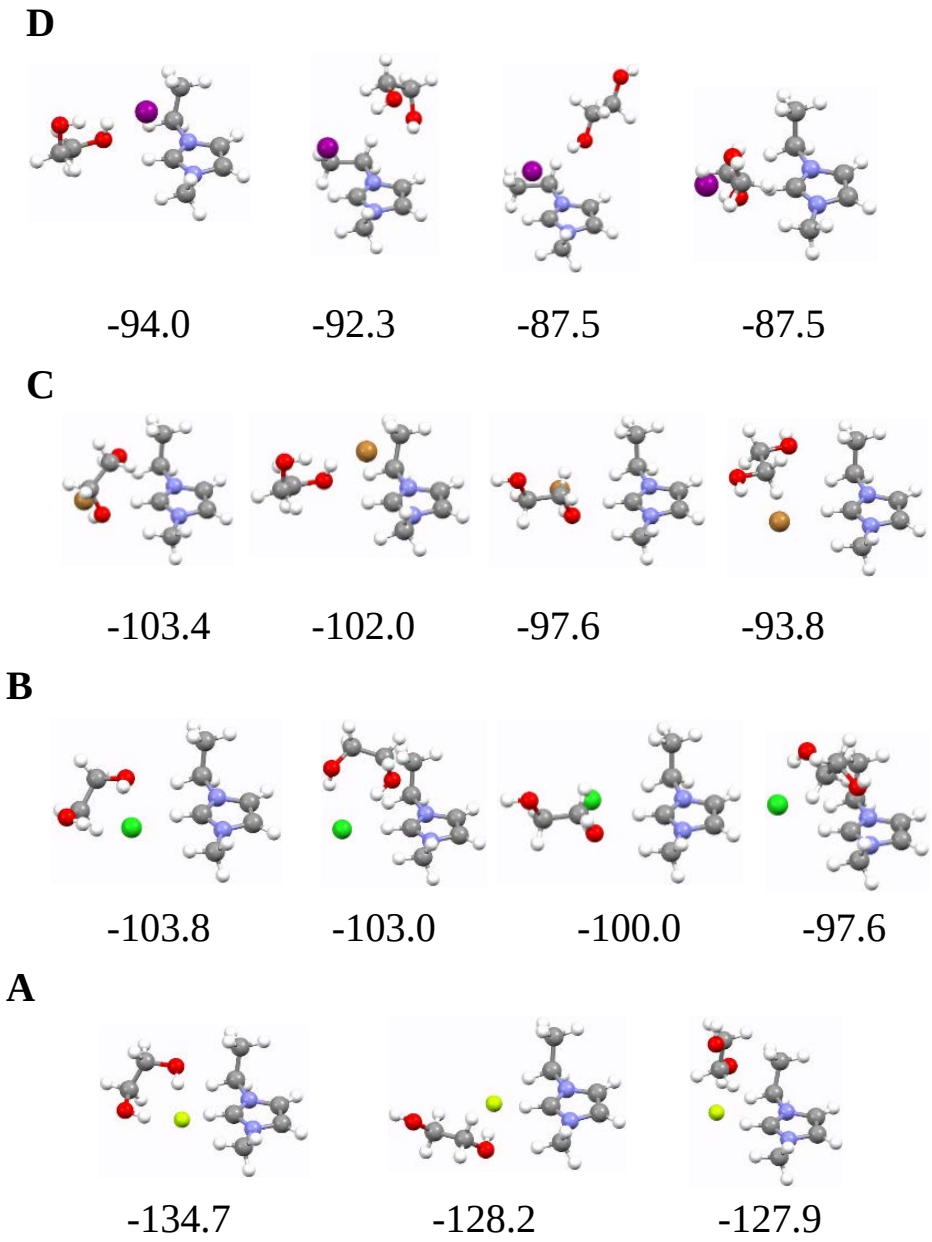

Figure 1. Optimized stable geometries of (A) [C_2C_1im]F·EG, (B) [C_2C_1im]Cl·EG, (C) [C_2C_1im]Br·EG, and (D) [C_2C_1im]I·EG complexes, and their stabilization energies by the formation of complexes in kcal mol^{-1}. Light green: fluorine, green: Cl, brown: Br, purple: I, blue: nitrogen, red: oxygen, gray: carbon, and white: hydrogen.

In Figure 2, the ^{1}H NMR spectra of neat [C_2C_1im]X·EG (to exclude solvent effects) with all peaks assigned are presented, in accordance with the previous work for the fluoride salt[24]. All methyl and ethyl hydrogen atoms (H6, H7, H8 and Ha) for these compounds have similar chemical shifts regardless of the anion, whereas the chemical shift of Hb (OH proton in EG) shows moderate downfield-shift from I^- to Cl^-, and then drastically for F^- as indicated by the arrows in Figure 2. The downfield shift of the proton in the NMR spectra is due to the increase of deshielding of protons by reinforcement of H-bonding[40], which is commonly observed in many other ionic liquids[33, 41, 42]. The changes of chemical shift are consistent with the calculated stabilization energies (Figure 1). The signal of the H2 ring proton also shifts downfield with decreasing the anion size in the same trend as for the OH proton, but in a moderate way. Slight downfield shift for the H4 and H5 ring protons are also observed from I^- to F^-, suggesting the increasing interaction with X^-.

This confirms that H2 receives the most significant effect of the anionic species in this system, which agrees with previous works suggesting the high acidity of H2[43-45]. The chemical shifts of H2 and Hb of [C_2C_1im]X·EG are plotted in Figure 3 against the Shannon radius[46] of X^-. The chemical shifts obtained by theoretical calculations are also shown for comparison (the values are listed in Table S1, Supplementary data). Although the calculated chemical shifts for the H2 and Hb protons are not identical to

the experimental values, the anion size dependency of the calculated chemical shifts is the same as that of the experimental chemical shifts. The F^- has the most significant influence on the H-bonding interactions owing to the strong interaction.

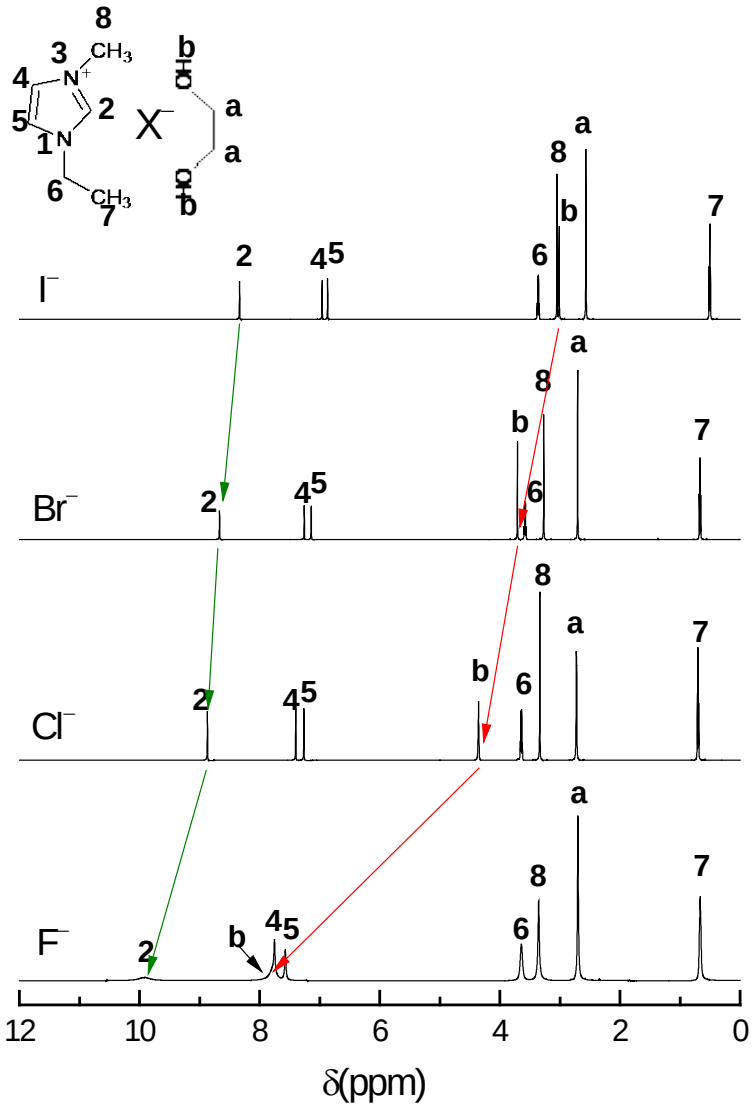

Figure 2. ^{1}H NMR spectra of $[C_2C_1im]X{\cdot}EG$ (X = F, Cl, Br and I) complexes at 20 °C. The arrows show the trend of the related chemical shift as function of anion size.

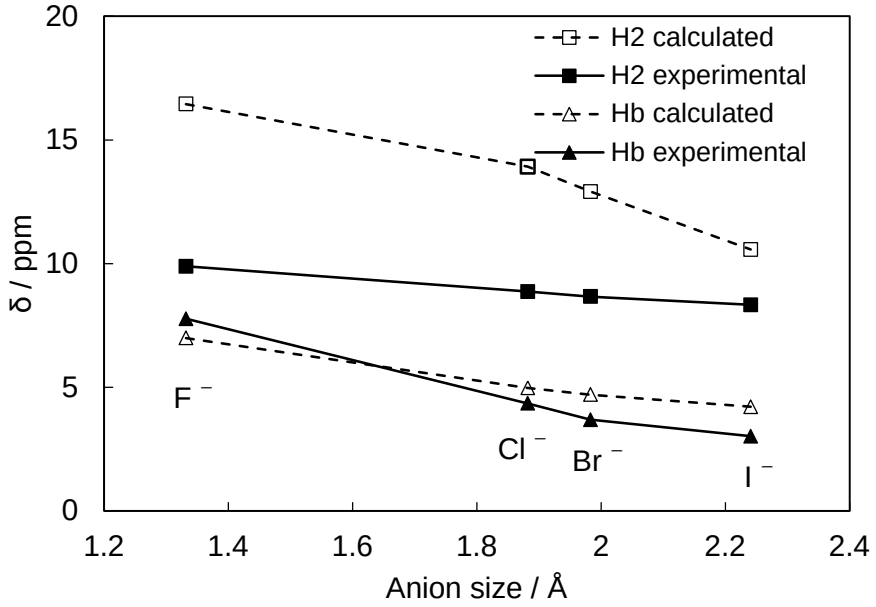

Figure 3. Calculated and experimental chemical shifts for the H2 (ring proton) and Hb (OH proton in EG) for the $[C_2C_1im]X{\cdot}EG$ (X = F, Cl, Br and I) complexes.

IR spectroscopy has been applied as a useful tool to study the H-bonding effect of the compound[47] in which the H-bonding would cause the related band to shift to lower wavenumber (red shift) and often a broadening effect[47-49]. Furthermore, IR is very sensitive to the state of OH stretching[50], which is the interaction of interest in the present study. IR spectra of the four $[C_2C_1im]X{\cdot}EG$ samples, neat EG and the neat $[C_2C_1im]Br$ salt are given in Figure 4. The OH stretching band of $[C_2C_1im]Cl{\cdot}EG$, $[C_2C_1im]Br{\cdot}EG$, and $[C_2C_1im]I{\cdot}EG$ appear at 3288, 3333, and 3371 cm^{-1}, respectively, exhibiting a blue shift with increasing the anion size. The larger wavenumber of these systems compared to that of neat EG (3265cm^{-1}) suggests that H-bonding in the complexes is weaker than that in neat EG, as EG forms oligomers via H bonding. The OH stretching band of $[C_2C_1im]F{\cdot}EG$ exhibits a distinct red-shift to 3035 cm^{-1}

compared to that of neat EG, indicative of the stronger H-bonding in the fluoride complex and the absence of "free" EG. The shift of the C−H stretching modes is rather ambiguous in the present spectra.

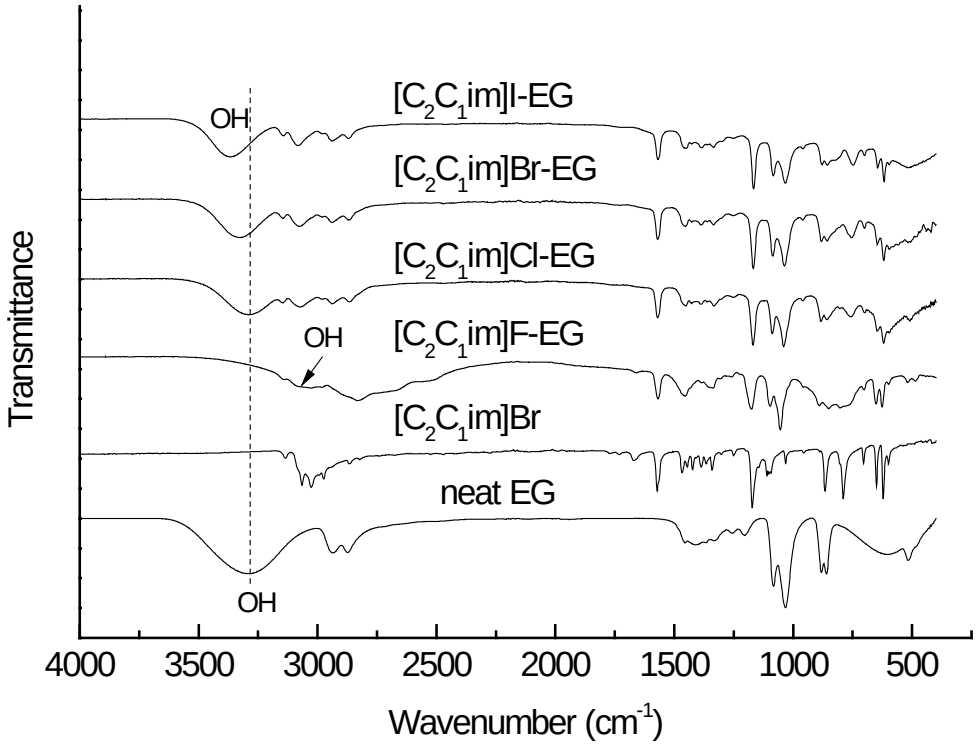

Figure 4. Infrared spectra of $[C_2C_1im]X{\cdot}EG$ (X = F, Cl, Br and I), $[C_2C_1im]Br$, and pure EG at 20 °C .

The difference in the H-bonding interactions is also reflected on their rheological behaviour, as stronger H-bonding interactions leading to a higher viscosity (η)[51]. The viscosities from 25 to 80 °C, of the $[C_2C_1im]X{\cdot}EG$ complex salts and neat EG are plotted in Figure S2. Any $[C_2C_1im]X{\cdot}EG$ salt exhibits a higher viscosity than that of neat EG, and the trend in viscosity, $\eta_{EG} < \eta_{I^-} < \eta_{Br^-} < \eta_{Cl^-} << \eta_{F^-}$, is in good accordance with the spectroscopic measurements. The decrease in viscosity is likely due to the

weaker anion-EG interaction (or partly increase of free EG) as similar to the case of other SILs[19, 22, 23]. The IR and rheological data suggest $[C_2C_1im]F{\cdot}EG$ can be considered as a “good” SIL based on the criteria for SILs[23].

2.2. ^1H-^2H exchange. In the imidazolium cations, the H2 ring hydrogen atom is the most acidic one which is subject to ^1H-^2H exchange in the presence of a deuterated solvent according to previous studies[33, 43], and the degree of exchange is largely affected by the anion type; the stronger interaction (mostly H-bonding) between the anion and H2 leads to the higher degree of ^1H-^2H exchange[33]. In the present $[C_2C_1im]X{\cdot}EG$ systems, thus, it is of fundamental importance to know the exchange phenomenon of these ^1H atoms in the presence of ^2H atoms. All the $[C_2C_1im]X{\cdot}EG$ complex salts were mixed with ^2H_2O in the molar ratio of 1 : 10 for 24 h and then ^1H_2O and ^2H_2O were removed under vacuum. The ^1H NMR spectra of the $[C_2C_1im]X{\cdot}EG$ after deuteration are presented in Figure 5. Although the chemical shifts do not change before and after deuteration (Figures 2 and 5), the intensities of Hb and H2 are significantly reduced in all cases, indicating that Hb and H2 have been partly deuterated. More strikingly, the intensities for H4 and H5 signals also decrease only in the case of $[C_2C_1im]F{\cdot}EG$ after deuteration, which agrees with a previous report[52], and is related to the formation of *N*-heterocyclic carbene. Formation of bifluoride ion is also a plausible path after abstraction of ring hydrogen atoms[30], but it was not observed in

IR spectra even in the case of the F^- system (absence of the characteristic band around 1250 cm^{-1} in Figure 4). This is the first case that shows the H4 and H5 hydrogen atoms exhibiting ^1H-^2H exchange in the presence of F^- at room temperature, although such deuteration could also be achieved under a basic conditions [45, 48].

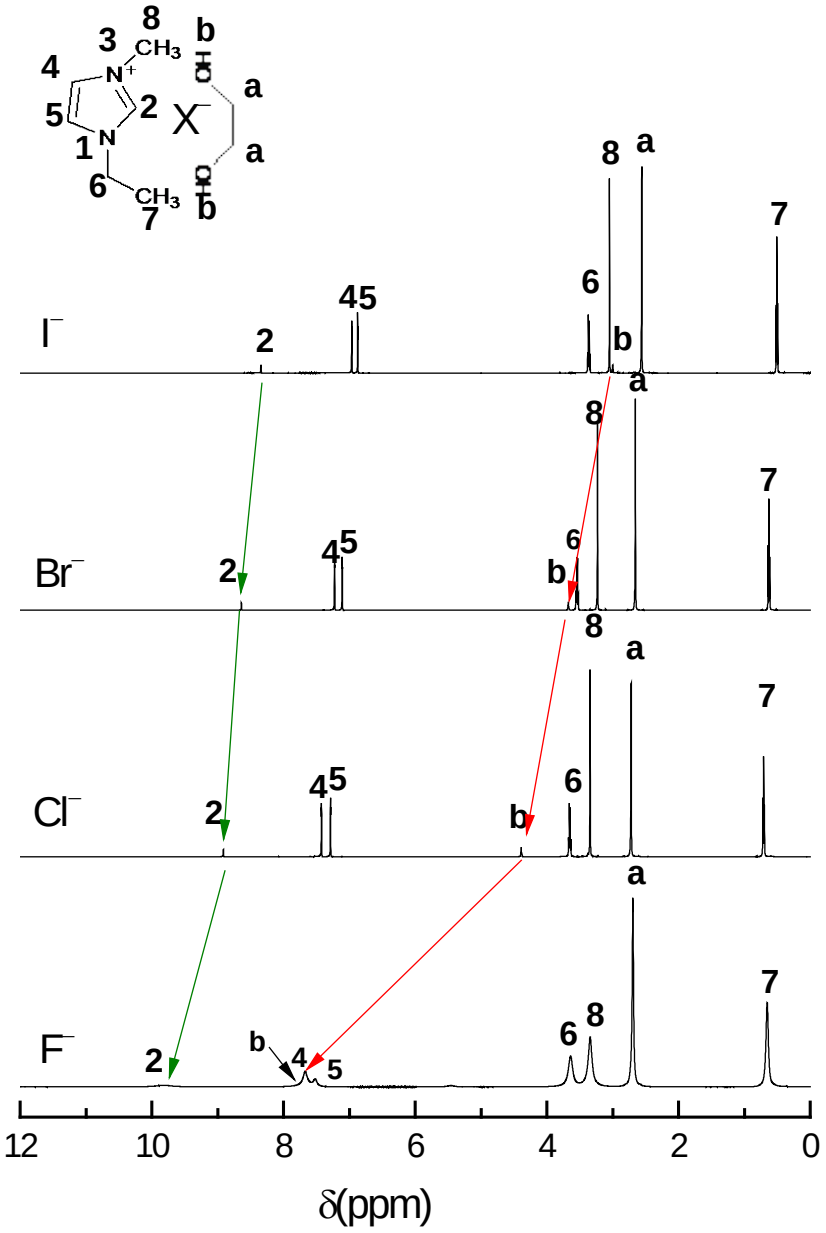

Figure 5. ^1H NMR spectra of $[C_2C_1im]X{\cdot}EG$ (X = F, Cl, Br, and I) after 24-hour deuteration with D_2O at 20 °C. The arrows show the trend of the chemical shift for Hb and H2 along with the change of anion.

The degree of ^{1}H-^{2}H exchange from the integration of the corresponding signals in ^{1}H NMR are given in Table 1 (detailed integrations for the protons are listed in Table S2, Supplementary data). The theoretical ^{1}H-^{2}H exchange rate for the Cl, Br, and I salts is 87 % at the equilibrated state based on the number of possible exchange sites (20/23 = 0.87 by considering three ^{1}H sites of one H2 and two Hb and twenty ^{2}H sites of $^{2}H_2O$ (ten $^{2}H_2O$ per $[C_2C_1im]X{\cdot}EG$)), whereas that for the F salt is 80 % (20/25 = 0.80 by considering five ^{1}H sites of H2, H4, H5, and two Hb, and twenty ^{2}H sites of $^{2}H_2O$ (ten $^{2}H_2O$ per $[C_2C_1im]X{\cdot}EG$)). The ^{1}H-^{2}H exchange rate experimentally observed for H2 and Hb in the Cl, Br and I salts are similar (84-88%) and close to the theoretical value, suggesting deuteration is almost completed in them. In the case of the F salt, the exchange rates are obviously different for H2, H4, H5, and Hb; the 77% exchange rate for H2 indicates almost completed ^{1}H-^{2}H exchange, whereas it decreases in the order of Hb > H4 = H5 (intensities of the H4 and H5 peaks were assumed to be identical to separate the H4 peak from the Hb peak).

^{1}H and ^{2}H atoms are electronically identical, and therefore the differences in the ^{1}H- and ^{2}H-bondings are associated with the difference in their masses, which is reflected on their zero-point energies. Table 2 lists the changes in zero-point energies due to the replacement of ^{1}H with ^{2}H in the $[C_2C_1im]X{\cdot}EG$, $[C_2C_1im]X$, and $[EG]X^{-}$ complexes.

The substitution of ^{1}H with ^{2}H lowers the energies of the complexes by about 2 kcal mol^{-1} regardless of the complex types. A similar difference of interaction energies between ^{1}H and ^{2}H complexes is reported in a water dimer[53]. This suggests that the ^{2}H-bonding is relatively more stable, meaning that the exchange between ^{1}H and ^{2}H atoms is promoted thermodynamically. However, the majority of ^{1}H atoms (especially those bonded to C atoms) are resistant to such an effect as reported in previous studies[33, 53-55]. In the imidazolium based salts ($[C_4C_1im]X$, X = Cl, Br, I and BF_4), the isotopic ^{1}H-^{2}H exchange for H2 hydrogen is also dependent on time, suggesting that the exchange can also be kinetically controlled[33]. To evaluate this kinetic effect, the deuteration time for the $[C_2C_1im]F{\cdot}EG$ and $[C_2C_1im]Cl{\cdot}EG$ samples was increased to three days. The resulting ^{1}H NMR spectra and integration numbers are given in Figure S3 and Table S2, respectively. The degree of deuteration for these two samples remains almost unchanged over a longer period, illustrating that the ^{1}H-^{2}H exchange reaches equilibrium after 24 h. Careful comparison of the difference in zero-point vibration energies (Table 2) indicates that the difference increases for H2 and decreases for Hb with increasing the anion size of $[C_2C_1im]X{\cdot}EG$. This trend results in the higher stability of deuterated Hb compared to deuterated H2 (-0.33 kcal mol^{-1}) for $[C_2C_1im]F{\cdot}EG$, but the overlap of Hb, H4, and H5 signals and broadness of H2 signal makes the accurate determination of intensities difficult in the current stage.

Table 1. Exchange rate of ^{1}H atoms with ^{2}H atoms in the $[C_2C_1im]X$-EG systems.[a]

IL	Hb/Db (%)	H2/D2 (%)	H4/D4 (%)	H5/D5 (%)
$[C_2C_1im]F\cdot EG$	67	77	56	56
$[C_2C_1im]Cl\cdot EG$	86	88	0	0
$[C_2C_1im]Br\cdot EG$	87	86	0	0
$[C_2C_1im]I\cdot EG$	85	84	0	0

[a] Deuteration was performed with $^{2}H_2O$ in the molar ratio of $[C_2C_1im]X$-EG : $^{2}H_2O$ = 1 : 10 and the percentage was determined by NMR spectroscopy (see Table S2 for NMR intensity data). The percentage is described as the atomic ratio of $^{2}H/(^{1}H + ^{2}H)$ for each hydrogen site.

Table 2. Change in zero-point vibration energy due to the replacement of ^{1}H with ^{2}H at H2 and Hb in $[C_2C_1im]X\cdot EG$, $[C_2C_1im]X$ and $[EG]X^-$ complexes.[a]

System	H2 (kcal mol^{-1})	Hb (kcal mol^{-1})
$[C_2C_1im]F\cdot EG$	-1.90	-2.23
$[C_2C_1im]Cl\cdot EG$	-2.00	-2.17
$[C_2C_1im]Br\cdot EG$	-2.03	-2.16
$[C_2C_1im]I\cdot EG$	-2.09	-2.14
$[C_2C_1im]F$	Unstable	--
$[C_2C_1im]Cl$	-1.88	--
$[C_2C_1im]Br$	-1.91	--
$[C_2C_1im]I$	-2.06	--
$F^-\cdots EG$	--	-2.14
$Cl^-\cdots EG$	--	-2.15
$Br^-\cdots EG$	--	-2.14
$I^-\cdots EG$	--	-2.14

[a]The difference in zero-point vibration energy between ^{1}H and ^{2}H forms is calculated by subtracting the energy of ^{2}H from that of ^{1}H.

In the optimized structure in Figure 1, F^- has short distances (Table S3) to Hb in EG and H2 in the imidazolium ring, giving rise to much stronger interactions compared to other halide counterparts. It is reasonably expected that F^- is also much closer to H4

and H5 in the ring than other halide ions. Consequently, these two ^{1}H atoms are more active (longer and weaker C-H bond) so that they could be exchanged by ^{2}H atoms in the presence of F^{-}. The ability of the strongly basic F^{-} to activate covalently bonded H atoms may be particularly useful in the event of deuteration of such compounds, since deuteration is a powerful tool to probe and tune H-bonded structures[21, 56-59], which may result in better crystal structure determination and design of new functional materials.

Due to the difference in the atomic mass between ^{1}H and ^{2}H, their vibrational energies are significantly different, which may be probed by spectroscopic techniques such as IR[33, 53, 60]. In the IR spectrum of deuterated EG (Figure S4, Supplementary data), the $O^{2}H$ stretching appears at a lower frequency of 2455 cm^{-1}, which is red-shifted by 837 cm^{-1}, compared to that of the non-deuterated EG (Figure 4). From the IR spectra of the $^{2}H_2O$ treated $[C_2C_1im]X{\cdot}EG$ samples, both $O^{1}H$ and $O^{2}H$ groups are observed, showing the similar isotopic shift (835 cm^{-1} for $[C_2C_1im]F{\cdot}EG$, 876 cm^{-1} for $[C_2C_1im]Cl{\cdot}EG$, 868 cm^{-1} for $[C_2C_1im]Br{\cdot}EG$, and 882 cm^{-1} for $[C_2C_1im]I{\cdot}EG$), in agreement with the NMR results that shows the co-existence of $O^{1}H$ and $O^{2}H$.

3. Conclusions

Four 1-ethyl-3-methylimidazolium halide-ethylene glycol mixtures ($[C_2C_1im]X{\cdot}EG$ (X=F, Cl, Br and I)) were systematically studied by computer simulations and

spectroscopic (NMR and IR) analyses. The quantum chemical calculations show that the halide ion being coordinated by EG in bidentate manner provides the most stable state for all the structures. In the absence of EG, [C_2C_1im]F is not stable as F^- abstracts the H2 atom on the imidazolium ring, whereas the other three complexes could form stable salts, which is consistent with experimental observations. Both ^{1}H NMR and IR analyses suggest that all the halide ions had interactions with the OH on EG and H2, H4 and H5 on the imidazole ring, but the strength of these interactions decreases in the trend of $F^- >> Cl^- > Br^- > I^-$ with the F^- being significantly higher than the others, which confirms the findings by the quantum chemical calculations. These microscopic structures have determined their macroscopic properties, such as viscosities measured in the present work. From the deuteration study, the ^{1}H-^{2}H exchange occurs for the OH and H2 hydrogen atoms in all the four systems, which is consistent with the previous literature. However, it is striking that H4 and H5 atoms could also be deuterated in the [C_2C_1im]F·EG system, due to these H atoms being activated by the strong basicity of F^- ion. This may be particularly useful in designing, synthesizing and analysing new materials, specifically those containing fluoride ions.

4. Experimental

4.1. General information

All non-volatile materials were handled under a dry Ar atmosphere in a glovebox. The starting halide salts, 1-ethyl-3-methylimidazolium halide ([C_2C_1im]X, X = Cl, Br and I), were purchased from Kanto Chemical Co. Inc. and were dried under vacuum at 50 °C overnight. Dry EG (Wako Pure Chemicals, water content < 30 ppm) and methanol (Wako Pure Chemicals, water content < 10 ppm) were used without further purification. Silver fluoride (Aldrich, 99% purity) was dried under vacuum overnight at 100 °C. Deuterium oxide (D_2O) was purchased from Aldrich (>99.9 at% D) and used as received.

4.2. Synthesis

[C_2C_1im]F·EG. The [C_2C_1im]F·EG compound was prepared using a protocol reported in a previous work[24]. Typically, [C_2C_1im]Br, AgF, and EG were mixed in methanol and agitated for 24 h. The precipitate of AgBr was filtered under the dry Ar atmosphere and the methanol solvent was evaporated from the filtrate at room temperature until the vacuum reached 1 Pa. The resulting [C_2C_1im]F·EG was yellow viscous liquid.

[C_2C_1im]X·EG (X = Cl, Br and I). The [C_2C_1im]X·EG (X = Cl, Br and I) were prepared via direct mixing of the corresponding halide salt and EG at the equimolar ratio for 1 h. The resulting product was clear liquid in all the cases, and the purities of

these compounds were confirmed by ^{1}H NMR with all peaks being assigned (see the Results and Discussion part).

^{1}H-^{2}H exchange. Each halide compound was mixed with $^{2}H_2O$ in the 1 : 10 molar ratio (e.g. 5.00 mmol [C_2C_1im]X·EG and 50.0 mmol D_2O) and was allowed for ^{1}H-^{2}H exchange for 24 h. Water ($^{1}H_2O$ or $^{2}H_2O$) was removed from the resulting mixture under vacuum at room temperature until the pressure reached 1 Pa, and the deuterated samples were then analyzed by ^{1}H NMR and IR spectroscopic measurements in their neat form to exclude solvent effects.

4.3. Characterization

The chemical structures of [C_2C_1im]X·EG complexes were analyzed by ^{1}H NMR on a JNM–ECA600 NMR spectrometer (JEOL Ltd.) at 20 °C. Neat liquid samples were used for the NMR measurements. A coaxial NMR tube was used with the sample being placed in the internal tube and the deuterated solvent in between to eliminate the interaction with the solvent. Infrared spectra were obtained by a Bruker Alpha II spectrometer equipped with an attenuated total reflection setup in a dry chamber (Daikin Industries, LTD.) under a dry air (dew point below –60 °C) at 25°C. Viscosity was measured using an electromagnetically spinning viscometer (EMS-1000, Kyoto

Electronics Manufacturing) from 25 to 80 °C. Samples for viscosity measurements were loaded in a glass tube in the glove box and was tightly sealed with a plastic cap.

4.4. Theoretical calculations

The Gaussian 09 program[61] was used for the *ab initio* molecular orbital and DFT calculations with the basis sets implemented in the Gaussian program. The DGDZVP basis set[62] was used for iodide. The geometries of the complexes were fully optimized at the HF/6-311G** level based on the previously known stable structures (two complex structures where X interacts with the H2 hydrogen atom and one complex structure where X^- is on the imidazolium ring)[63, 64]. The intermolecular interaction energies (E_{int}) were calculated at the MP2/6-311G** level by the supermolecule method[65, 66]. The basis set superposition error (BSSE)[67] was corrected for all the interaction energy calculations using the counterpoise method[68]. The previous calculations of the $[C_2C_1im][BF_4]$ and Li[TFSA] complexes[69, 70] show that the basis set effects on the calculated interaction energies of the complexes are very small, if basis sets including polarization functions are used and that the effects of electron correlation beyond MP2 are negligible. Therefore, we calculated the interaction energies of the complexes at the MP2/6-311G** level in this work. The stabilization energy for forming a complex from the isolated species (E_{form}) was calculated as the

sum of the E_{int} and the deformation energy (E_{def}), which is the sum of the increase in energy due to the deformation of the chemical species during formation of the complex[70]. Here, the E_{def} was calculated at the MP2/6-311G** level. NMR shielding tensors were calculated with the Gauge-independent atomic orbital (GIAO) method[71] from the B3LYP/6-311+G** level[72, 73] wave functions calculated for the optimized geometries at the same level. Zero point vibrational energies were calculated at the B3LYP/6-311+G** level.

Declaration of Competing Interest

The authors declare no competing financial interest.

Acknowledgments

Z.C. acknowledges the International Fellowship (P17717) from the Japan Society for the Promotion of Science (JSPS) and the Start-up Fund from Ningbo Institute of Technology, Zhejiang University (20190709Z0078). The NMR measurements were supported by the Joint Usage/Research Program on Zero-Emission Energy Research, Institute of Advanced Energy, Kyoto University (ZE2020A-25). The authors thank Dr. Masayuki Saimura (Institute of Advanced Energy, Kyoto University) for his help on

NMR measurements. This work was financially supported by the Grant-in-Aid for Scientific Research (17F17717).

Appendix A. Supplementary data

Supplementary materials related to this article can be found, in the online version, at XXXX.

■ References

[1] T. Welton, Ionic liquids in catalysis, Coord. Chem. Rev. 248 (2004) 2459-2477.
[2] J.P. Hallett, T. Welton, Room-temperature ionic liquids: Solvents for synthesis and catalysis. 2, Chem. Rev. 111 (2011) 3508-3576.
[3] R. Hagiwara, Y. Ito, Room temperature ionic liquids of alkylimidazolium cations and fluoroanions, J. Fluorine Chem. 105 (2000) 221-227.
[4] H. Xue, R. Verma, M.S. Jean'ne, Review of ionic liquids with fluorine-containing anions, J. Fluorine Chem. 127 (2006) 159-176.
[5] Y. Zhou, M. Antonietti, A series of highly ordered, super-microporus, lamellar silicas prepared by nanocasting with ionic liquids, Chem. Mater. 16 (2004) 544-550.
[6] Y. Zhou, J.H. Schattka, M. Antonietti, Room-temperature ionic liquids as template to monolithic mesoporous silica with wormlike pores via a sol-gel nanocasting technique, Nano Lett. 4 (2004) 477-481.
[7] A. Pinkert, K.N. Marsh, S.S. Pang, M.P. Staiger, Ionic liquids and their interaction with cellulose, Chem. Rev. 109 (2009) 6712-6728.
[8] V.I. Parvulescu, C. Hardacre, Catalysis in ionic liquids, Chem. Rev. 107 (2007) 2615-2665.
[9] T.L. Greaves, A. Weerawardena, C. Fong, C.J. Drummond, Formation of amphiphile self-assembly phases in protic ionic liquids, J. Phys. Chem. B 111 (2007) 4082-4088.
[10] T.L. Greaves, A. Weerawardena, I. Krodkiewska, C.J. Drummond, Protic ionic liquids: Physicochemical properties and behavior as amphiphile self-assembly solvents, J. Phys. Chem. B 112 (2008) 896-905.
[11] M. Galinski, A. Lewandowski, I. Stepniak, Ionic liquids as electrolytes, Electrochim. Acta 51 (2006) 5567-5580.
[12] M. Watanabe, M.L. Thomas, S. Zhang, K. Ueno, T. Yasuda, K. Dokko, Application of ionic liquids to energy storage and conversion materials and devices, Chem. Rev. 117 (2017)

7190-7239.
[13] Y. Zhao, T. Bostrom, Application of ionic liquids in solar cells and batteries: A review, Curr. Org. Chem. 19 (2015) 556-566.
[14] H. Ohno, Electrochemical aspects of ionic liquids, 2nd edn., John Wiley & Sons, Hoboken, NJ, 2011.
[15] C. Austen Angell, Y. Ansari, Z. Zhao, Ionic liquids: Past, present and future, Faraday Discuss. 154 (2012) 9-27.
[16] T. Tamura, K. Yoshida, T. Hachida, M. Tsuchiya, M. Nakamura, Y. Kazue, N. Tachikawa, K. Dokko, M. Watanabe, Physicochemical properties of glyme–li salt complexes as a new family of room-temperature ionic liquids, Chem. Lett. 39 (2010) 753-755.
[17] W.A. Henderson, N.R. Brooks, W.W. Brennessel, V.G. Young, Triglyme–li+ cation solvate structures: Models for amorphous concentrated liquid and polymer electrolytes (i), Chem. Mater. 15 (2003) 4679-4684.
[18] K. Ueno, R. Tatara, S. Tsuzuki, S. Saito, H. Doi, K. Yoshida, T. Mandai, M. Matsugami, Y. Umebayashi, K. Dokko, M. Watanabe, Li+ solvation in glyme-li salt solvate ionic liquids, Phys. Chem. Chem. Phys. 17 (2015) 8248-8257.
[19] K. Ueno, K. Yoshida, M. Tsuchiya, N. Tachikawa, K. Dokko, M. Watanabe, Glyme–lithium salt equimolar molten mixtures: Concentrated solutions or solvate ionic liquids?, J. Phys. Chem. B 116 (2012) 11323-11331.
[20] Y. Marcus, G. Hefter, Ion pairing, Chem. Rev. 106 (2006) 4585-4621.
[21] T. Murphy, S.K. Callear, N. Yepuri, K. Shimizu, M. Watanabe, J.N. Canongia Lopes, T. Darwish, G.G. Warr, R. Atkin, Bulk nanostructure of the prototypical 'good' and 'poor' solvate ionic liquids [li(g4)][tfsi] and [li(g4)][no3], Phys. Chem. Chem. Phys. 18 (2016) 17224-17236.
[22] K. Shimizu, A.A. Freitas, R. Atkin, G.G. Warr, P.A. FitzGerald, H. Doi, S. Saito, K. Ueno, Y. Umebayashi, M. Watanabe, J.N. Canongia Lopes, Structural and aggregate analyses of (li salt + glyme) mixtures: The complex nature of solvate ionic liquids, Phys. Chem. Chem. Phys. 17 (2015) 22321-22335.
[23] T. Mandai, K. Yoshida, K. Ueno, K. Dokko, M. Watanabe, Criteria for solvate ionic liquids, Phys. Chem. Chem. Phys. 16 (2014) 8761-8772.
[24] Z. Chen, Y. Tonouchi, K. Matsumoto, M. Saimura, R. Atkin, T. Nagata, M. Katahira, R. Hagiwara, Partially naked fluoride in solvate ionic liquids, J. Phys. Chem. Lett. 9 (2018) 6662-6667.
[25] C.R. Ashworth, R.P. Matthews, T. Welton, P.A. Hunt, Doubly ionic hydrogen bond interactions within the choline chloride-urea deep eutectic solvent, Phys. Chem. Chem. Phys. 18 (2016) 18145-18160.
[26] R. Stefanovic, M. Ludwig, G.B. Webber, R. Atkin, A.J. Page, Nanostructure, hydrogen

bonding and rheology in choline chloride deep eutectic solvents as a function of the hydrogen bond donor, Phys. Chem. Chem. Phys. 19 (2017) 3297-3306.
[27] K.O. Christe, H.D. Brooke Jenkins, Quantitative measure for the “nakedness” of fluoride ion sources J. Am. Chem. Soc. 125 (2003) 14210-14210.
[28] K.O. Christe, W.W. Wilson, R.D. Wilson, R. Bau, J.A. Feng, Syntheses, properties, and structures of anhydrous tetramethylammonium fluoride and its 1:1 adduct with trans-3-amino-2-butenenitrile, J. Am. Chem. Soc. 112 (1990) 7619-7625.
[29] H. Sun, S.G. DiMagno, Anhydrous tetrabutylammonium fluoride, J. Am. Chem. Soc. 127 (2005) 2050-2051.
[30] B. Ališ, G. Tavčar, Reaction of n-heterocyclic carbene (nhc) with different hf sources and ratios – a free fluoride reagent based on imidazolium fluoride, J. Fluorine Chem. 192 (2016) 141-146.
[31] J.-W. Lee, M.T. Oliveira, H.B. Jang, S. Lee, D.Y. Chi, D.W. Kim, C.E. Song, Hydrogen-bond promoted nucleophilic fluorination: Concept, mechanism and applications in positron emission tomography, Chem. Soc. Rev. 45 (2016) 4638-4650.
[32] K.M. Engle, L. Pfeifer, G.W. Pidgeon, G.T. Giuffredi, A.L. Thompson, R.S. Paton, J.M. Brown, V. Gouverneur, Coordination diversity in hydrogen-bonded homoleptic fluoride–alcohol complexes modulates reactivity, Chem. Sci. 6 (2015) 5293-5302.
[33] S. Cha, M. Ao, W. Sung, B. Moon, B. Ahlström, P. Johansson, Y. Ouchi, D. Kim, Structures of ionic liquid–water mixtures investigated by ir and nmr spectroscopy, Phys. Chem. Chem. Phys. 16 (2014) 9591-9601.
[34] G. Cheng, W.W. Graessley, Y.B. Melnichenko, Polymer dimensions in good solvents: Crossover from semidilute to concentrated solutions, Phys. Rev. Lett. 102 (2009) 157801.
[35] G.D. Wignall, Y.B. Melnichenko, Recent applications of small-angle neutron scattering in strongly interacting soft condensed matter, Rep. Prog. Phys. 68 (2005) 1761-1810.
[36] R. Atkin, G.G. Warr, The smallest amphiphiles: Nanostructure in protic room-temperature ionic liquids with short alkyl groups, J. Phys. Chem. B 112 (2008) 4164-4166.
[37] Z. Chen, P.A. FitzGerald, Y. Kobayashi, K. Ueno, M. Watanabe, G.G. Warr, R. Atkin, Micelle structure of novel diblock polyethers in water and two protic ionic liquids (ean and pan), Macromolecules 48 (2015) 1843-1851.
[38] Z. Chen, P.A. FitzGerald, G.G. Warr, R. Atkin, Conformation of poly(ethylene oxide) dissolved in the solvate ionic liquid [li(g4)]tfsi, Phys. Chem. Chem. Phys. 17 (2015) 14872-14878.
[39] T. Murphy, R. Hayes, S. Imberti, G.G. Warr, R. Atkin, Nanostructure of an ionic liquid-glycerol mixture, Phys. Chem. Chem. Phys. 16 (2014) 13182-13190.
[40] J.E. Del Bene, S.A. Perera, R.J. Bartlett, Hydrogen bond types, binding energies, and 1h nmr chemical shifts, J. Phys. Chem. A 103 (1999) 8121-8124.
[41] S. Chen, R. Vijayaraghavan, D.R. MacFarlane, E.I. Izgorodina, Ab initio prediction of

proton nmr chemical shifts in imidazolium ionic liquids, J. Phys. Chem. B 117 (2013) 3186-3197.
[42] P.A. Hunt, C.R. Ashworth, R.P. Matthews, Hydrogen bonding in ionic liquids, Chem. Soc. Rev. 44 (2015) 1257-1288.
[43] T.L. Amyes, S.T. Diver, J.P. Richard, F.M. Rivas, K. Toth, Formation and stability of n-heterocyclic carbenes in water: The carbon acid pka of imidazolium cations in aqueous solution, J. Am. Chem. Soc. 126 (2004) 4366-4374.
[44] C.J. Dymek, D.A. Grossie, A.V. Fratini, W. Wade Adams, Evidence for the presence of hydrogen-bonded ion-ion interactions in the molten salt precursor, 1-methyl-3-ethylimidazolium chloride, J. Mol. Struct. 213 (1989) 25-34.
[45] N. Hayashi, H. Kuyama, C. Nakajima, K. Kawahara, M. Miyagi, O. Nishimura, H. Matsuo, T. Nakazawa, Imidazole c-2 hydrogen/deuterium exchange reaction at histidine for probing protein structure and function with matrix-assisted laser desorption ionization mass spectrometry, Biochemistry 53 (2014) 1818-1826.
[46] R. Shannon, Revised effective ionic radii and systematic studies of interatomic distances in halides and chalcogenides, Acta Crystallographica Section A 32 (1976) 751-767.
[47] S.J. Barlow, G.V. Bondarenko, Y.E. Gorbaty, T. Yamaguchi, M. Poliakoff, An ir study of hydrogen bonding in liquid and supercritical alcohols, J. Phys. Chem. A 106 (2002) 10452-10460.
[48] K.M. Dieter, C.J. Dymek, N.E. Heimer, J.W. Rovang, J.S. Wilkes, Ionic structure and interactions in 1-methyl-3-ethylimidazolium chloride-aluminum chloride molten salts, J. Am. Chem. Soc. 110 (1988) 2722-2726.
[49] S. Tait, R.A. Osteryoung, Infrared study of ambient-temperature chloroaluminates as a function of melt acidity, Inorg. Chem. 23 (1984) 4352-4360.
[50] K. Krishnan, R.S. Krishnan, Raman and infrared spectra of ethylene glycol, Proceedings of the Indian Academy of Sciences - Section A 64 (1966) 111.
[51] J.A. Smith, G.B. Webber, G.G. Warr, R. Atkin, Rheology of protic ionic liquids and their mixtures, J. Phys. Chem. B 117 (2013) 13930-13935.
[52] E.M. Higgins, Proton transfer at carbon, Department of Chemistry, Durham University, Durham, 2007, p. 372.
[53] S. Scheiner, M. Čuma, Relative stability of hydrogen and deuterium bonds, J. Am. Chem. Soc. 118 (1996) 1511-1521.
[54] A. Grimison, The deuterium isotope effect in the hydrogen bonding of imidazole in naphthalene solutions, J. Phys. Chem. 67 (1963) 962-964.
[55] C.N.R. Rao, Effect of deuteration on hydrogen bonds, Journal of the Chemical Society, Faraday Transactions 1: Physical Chemistry in Condensed Phases 71 (1975) 980-983.
[56] C. Shi, X. Zhang, C.-H. Yu, Y.-F. Yao, W. Zhang, Geometric isotope effect of deuteration

in a hydrogen-bonded host–guest crystal, Nature Communications 9 (2018) 481.
[57] R. Hayes, S.Z. El Abedin, R. Atkin, Pronounced structure in confined aprotic room-temperature ionic liquids, J. Phys. Chem. B 113 (2009) 7049-7052.
[58] R. Hayes, S. Imberti, G.G. Warr, R. Atkin, Amphiphilicity determines nanostructure in protic ionic liquids, Phys. Chem. Chem. Phys. 13 (2011) 3237-3247.
[59] R. Hayes, G.G. Warr, R. Atkin, Structure and nanostructure in ionic liquids, Chem. Rev. 115 (2015) 6357-6426.
[60] A.D. Buckingham, L. Fan-Chen, Differences in the hydrogen and deuterium bonds, Int. Rev. Phys. Chem. 1 (1981) 253-269.
[61] M.J. Frisch, G.W. Trucks, H.B. Schlegel, G.E. Scuseria, M.A. Robb, J.R. Cheeseman, G. Scalmani, V. Barone, G.A. Petersson, H. Nakatsuji, X. Li, M. Caricato, A.V. Marenich, J. Bloino, B.G. Janesko, R. Gomperts, B. Mennucci, H.P. Hratchian, J.V. Ortiz, A.F. Izmaylov, J.L. Sonnenberg, Williams, F. Ding, F. Lipparini, F. Egidi, J. Goings, B. Peng, A. Petrone, T. Henderson, D. Ranasinghe, V.G. Zakrzewski, J. Gao, N. Rega, G. Zheng, W. Liang, M. Hada, M. Ehara, K. Toyota, R. Fukuda, J. Hasegawa, M. Ishida, T. Nakajima, Y. Honda, O. Kitao, H. Nakai, T. Vreven, K. Throssell, J.A. Montgomery Jr., J.E. Peralta, F. Ogliaro, M.J. Bearpark, J.J. Heyd, E.N. Brothers, K.N. Kudin, V.N. Staroverov, T.A. Keith, R. Kobayashi, J. Normand, K. Raghavachari, A.P. Rendell, J.C. Burant, S.S. Iyengar, J. Tomasi, M. Cossi, J.M. Millam, M. Klene, C. Adamo, R. Cammi, J.W. Ochterski, R.L. Martin, K. Morokuma, O. Farkas, J.B. Foresman, D.J. Fox, Gaussian 16 rev. C.01, Gaussian Inc. Wallingford CT (2009).
[62] N. Godbout, D.R. Salahub, J. Andzelm, E. Wimmer, Optimization of gaussian-type basis sets for local spin density functional calculations. Part i. Boron through neon, optimization technique and validation, Can. J. Chem. 70 (1992) 560-571.
[63] S. Tsuzuki, A.A. Arai, K. Nishikawa, Conformational analysis of 1-butyl-3-methylimidazolium by ccsd(t) level ab initio calculations: Effects of neighboring anions, J. Phys. Chem. B 112 (2008) 7739-7747.
[64] S. Tsuzuki, R. Katoh, M. Mikami, Analysis of interactions between 1-butyl-3-methylimidazolium cation and halide anions (cl−, br− and i−) by ab initio calculations: Anion size effects on preferential locations of anions, Mol. Phys. 106 (2008) 1621-1629.
[65] C. Møller, M.S. Plesset, Note on an approximation treatment for many-electron systems, Phys. Rev. A 46 (1934) 618-622.
[66] M. Headgordon, J. Pople, M. Frisch, Mp2 energy evaluation by direct methods, Chem. Phys. Lett. 153 (1988) 503-506.
[67] B.J. Ransil, Studies in molecular structure. Iv. Potential curve for the interaction of two helium atoms in single-configuration lcao mo scf approximation, Journal of Chemical Physics 34 (1961) 2109-2118.
[68] S.F. Boys, F. Bernardi, Calculation of small molecular interactions by differences of

separation total energies-some procedures with reduced errors, Mol. Phys. 19 (1970) 553-566.
[69] S. Tsuzuki, H. Tokuda, K. Hayamizu, M. Watanabe, Magnitude and directionality of interaction in ion pairs of ionic liquids: Relationship with ionic conductivity, J Journal of Physical Chemistry B 109 (2005) 16474-16481.
[70] S. Tsuzuki, K. Hayamizu, S. Seki, Y. Ohno, Y. Kobayashi, H. Miyashiro, Quaternary ammonium room-temperature ionic liquid including an oxygen atom in side chain/lthium slt bnary electrolytes: Ab initio molecular orbital calculations of interactions between ions, J. Phys. Chem. B 112 (2008) 9914-9920.
[71] K. Wolinski, J.F. Hinton, P. Pulay, Efficient implementation of the gauge-independent atomic orbital method for nmr chemical shift calculations, J. Am. Chem. Soc. 112 (1990) 8251-8260.
[72] C. Lee, W. Yang, R.G. Parr, Development of the colle-salvetti correlation-energy formula into a functional of the electron density, Phys. Rev. B 37 (1988) 785-789.
[73] A.D. Becke, Density-functional thermochemistry. Iii. The role of exact exchange, J. Chem. Phys. 98 (1993) 5648-5652.